THE JOURNAL OF PHYSICAL CHEMISTRY B

pubs.acs.org/JPCB Article

Path-Dependent Self-Assembly of Magnetic Anisotropic Colloidal Peanuts

Md. Arif Kamal, Andrei V. Petukhov, and Antara Pal*

Cite This: *J. Phys. Chem. B* 2020, 124, 5754–5760 Read Online

ACCESS | Metrics & More | Article Recommendations | Supporting Information

ABSTRACT: Here we present the field induced self-assembly of anisotropic colloidal particles whose shape resembles peanuts. Being made up of hematite core and silica shell, these particles align in a direction perpendicular to the applied external magnetic field. Using small-angle X-ray scattering with microradian resolution (μrad-SAXS) in sedimented samples, we have found that one can tune the self-assembled structures by changing the time of application of the external field. If the field is applied after the sedimentation, the self-assembled structure is a nematic one, while dipolar chains are formed if the field is applied during the sedimentation process. Interestingly, within each chain particles form a smectic phase with defects. Further, these aforementioned nematic and smectic phases are of oblate type in spite of the prolate shape of the individual particles. For dipolar chains, an unusual diffraction peak shape has been observed with highly anisotropic tails in the transverse direction (perpendicular to the external field). The peak shape can be rationalized by considering the fact that the dipolar chains can act as a building block aligned along the field direction to form a para-nematic phase.

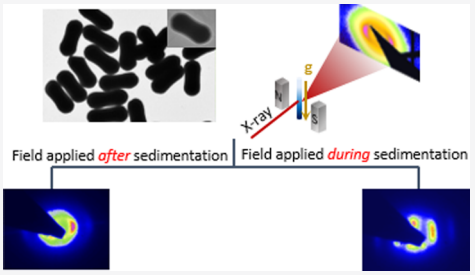

INTRODUCTION

The ability to manipulate the self-assembly in colloidal systems has opened up an alternative route toward the development of smart materials with designable properties.[1,2] As a result, a considerable amount of research has been carried out over the last couple of decades to understand as well as to manipulate the self-assembled structures formed by colloidal particles possessing basic shapes like spheres,[3,4] rods,[5−7] disks,[8] and ellipsoids.[9,10] Recent progress in the synthetic techniques of colloidal particles has resulted in the fabrication of particles with complex shapes resembling peanuts,[11−13] dumbbells,[14−16] polyhedras,[17,18] and octapods,[19] to name but a few. Controlling the self-assembly of these particles requires a thorough control over the interparticle interactions. Additionally, there are some other major challenges that also need to be overcome—control over particle orientation, their localization, and their registry into self-assembled structures. Therefore, the possibility to explore the different self-assembled structures formed from diverse complex building blocks has contributed significantly toward reinvigorating colloidal science in recent times.

One of the simplest ways to regulate the self-assembly process is through an external stimulus. Of all the different colloidal particles that can in principle be manipulated using external stimuli, magnetic colloids have attracted much attention. The primary reason behind this is the fast and reversible nature of the dipole−dipole interactions together with their wide-ranging applicability in diverse fields including photonics,[20,21] drug delivery,[22,23] patterning,[24,25] and magnetic levitation,[26,27] to name but a few. In order to fully exploit the potential of stimuli responsive self-assembled structures, one needs to understand not only the final structure but also the kinetics of the self-assembly processes. Thus, acquired knowledge would be particularly helpful in avoiding the undesirable metastable phases that might restrict the possibility of obtaining the desired smart synthetic materials. Understanding the path dependent self-assembly process will have wider implications on different areas of science and engineering, e.g., condensed matter physics and metallurgy, with impact on applications that range from obtaining tailor-made metallic alloys and ceramics to modern shape-memory materials.[28,29]

In this article, we present our investigations on the stimuli responsive self-assembly of micron-sized anisotropic peanut-shaped colloids in sedimented samples using μrad-SAXS. Sedimentation has been used with an intention to efficiently sample the phase behavior of these particles as a function of packing fraction. Being made up of hematite core and silica shell, they orient with their long axes in planes perpendicular to the field direction. We demonstrate that the self-assembled structures strongly depend on when the external field is switched on—*during* or *after* the sedimentation process. When the field is applied *after* sedimentation, an *oblate* nematic phase

Received: April 28, 2020
Revised: June 9, 2020
Published: June 9, 2020

https://dx.doi.org/10.1021/acs.jpcb.0c03771
J. Phys. Chem. B 2020, 124, 5754–5760

results with the nematic director oriented along the short axes of the particles. However, the scenario changes drastically once the field is applied during the sedimentation process. In the latter case, dipolar chains form due to the dipole−dipole interaction between the particles. In addition, we also observed a peculiar stretching of the diffraction peaks perpendicular to the direction of the dipolar chains. We believe that in this case the dipolar chains can act as elongated building blocks which align along the field direction to form a para-nematic phase. Owing to the large particle size and high density, their gravitational length is quite small; as a result, we did not observe any variation in the self-assembled structures as a function of sedimentation height.

SYNTHESIS AND CHARACTERIZATION METHODS

Synthesis. Micron-sized hematite peanuts were synthesized following the sol−gel method proposed by Sugimoto et al.[30] In a typical synthesis, 90 mL of 6.0 M NaOH (Merck) was slowly added in approximately 5 min to 100 mL of a magnetically stirred 2.0 M $FeCl_3$ (Sigma-Aldrich, puriss. p.a.) solution followed by the addition of 10 mL of a 0.25 M Na_2SO_4 (Acros, 99%) solution. Subsequently, the obtained condensed iron hydroxide gel was aged at 100 °C for 8 days. The resulting precipitated particles were then purified by repeated centrifugation and redispersion cycles in water.

In the next step, the hematite particles were coated with an additional silica layer by following Graf et al.[31] As an initial step, the particles were coated with a sterically stabilizing layer by adding excess of PVP to an aqueous hematite particle dispersion while stirring. The dispersion was stirred overnight and finally was washed with ethanol. The silica coating was performed in a 3 L round-bottom flask under mechanical stirring and ultrasonication. A mixture of 1 L ethanol, 100 mL water, and 10 mL of a 1 wt % TMAH solution was prepared and 10 g of 10 wt % PVP-stabilized hematite dispersion in ethanol was added. Subsequently, TEOS solutions were added using a peristaltic pump operating at 16 mL/h. The TEOS solution was prepared by mixing 10 mL of TEOS and 10 mL of ethanol. To prevent aggregation, a solution of 20 g PVP in 100 mL water was added to the dispersion, which was then sonicated for 2 more hours and stirred overnight. The silica-coated particle dispersion was washed several times with ethanol and then with water.

Characterization Methods. The size and shape of the peanut-shaped colloidal particles were characterized using transmission electron microscopy (TEM) (Philips TECNAI 10) (Figure 1a). The length of the particles and the diameter of their lobes are found to be 1723 ± 50 nm and 740 ± 50 nm, respectively, by analyzing more than 100 particles in the TEM images.

For SAXS measurements, dispersions of peanuts ∼5 wt % were placed in capillaries with internal dimensions of 100 × 4 × 0.2 mm^3 (W3520 Vitrocom) that were flame-sealed and stored vertically and left undisturbed for 24 h for particle sedimentation. In order to investigate the self-assembled structures, the sedimentation profiles were scanned over the full length of the capillary along the vertical directions while $Z = 0$ was set at the bottom of the capillaries. SAXS measurements were performed at BM26B beamline at ESRF, Grenoble. We have employed a μrad-SAXS setup which involves compound refractive lenses.[32] The 13 kev X-ray beam was focused on a CCD X-ray detector which was placed at a distance of 7.45 m from the samples. The data have been

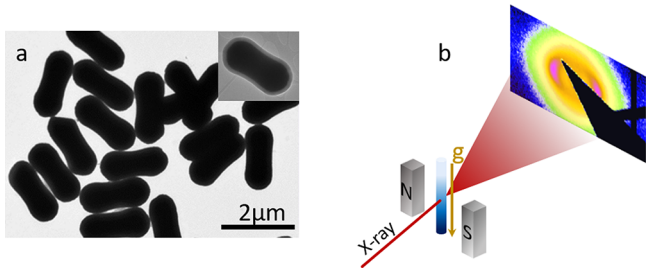

Figure 1. (a) Representative TEM image of silica coated hematite peanut shaped particles. (b) Experimental scheme for the SAXS experiment. In this case, the X-ray beam, external magnetic field direction, and the direction of gravity are perpendicular to each other.

recorded with a Photonic science detector with pixel size of 24 × 24 μm^2. The detector was protected from the direct X-ray beam using a wedge-shaped beam-stop that shades the detector. The capillaries were oriented vertically with their length (100 mm) parallel to the gravitational field. All the measurements were carried out in the presence of external magnetic fields which were applied using a permanent magnet. The direction of the magnetic field (B), X-ray beam, and gravity were perpendicular to each other as shown in Figure 1b.

RESULTS AND DISCUSSION

The self-assembly of peanut shaped colloidal particles was studied in the presence of external magnetic fields under two different conditions. In the first case, the magnetic field was applied after the sedimentation process was over, whereas in the second case, the field was applied while the particles were still sedimenting. Interestingly, the subsequent self-assembled structures exhibited a strong dependence upon when the field was applied as discussed in the following subsections.

Route 1: Application of the Magnetic Field *after* Sedimentation. In this case, the filled-in capillaries were stored vertically unperturbed for 24 h. Once the particles had formed thick sedimented layers, magnetic fields of different magnitudes were applied and the measurements were done. For all the magnetic fields measured (12.3 mT ≤ B ≤ 380 mT), we found nicely ordered nematic phases, the representative diffraction pattern of which is shown in Figure 2a. However, the aforementioned nematic phase is quite different from that normally observed for rod-like objects.[5−7] For colloidal rods, a nematic phase is expected when $L/D >$ 3.4.[33] In addition, the nematic order for this phase is expected to be along the *long axes* of the particles. In the present case, although the $L/D \sim 2.3$, we still observe a nematic phase in the presence of an external field. However, in the absence of external field, we observe an isotropic phase as expected, which does not show any variation in the nearest neighbor distance as a function of height from the bottom of the capillary (Supporting Information). Further, the nematic order of the field induced self-assembled phase is along the *short axes* of the particles. From that point of view, this nematic phase is similar to the one that is observed for colloidal platelets where the nematic director is along the short axes of the particles.[8] In a nutshell, one can say that although the particles are *prolate* in shape, the nematic phase formed by them has the characteristics of the one formed by *oblate* particles. Having obtained similar results for colloidal ellipsoids (unpublished results) leads us to a conclusion that the aforementioned feature seems

https://dx.doi.org/10.1021/acs.jpcb.0c03771
J. Phys. Chem. B 2020, 124, 5754−5760

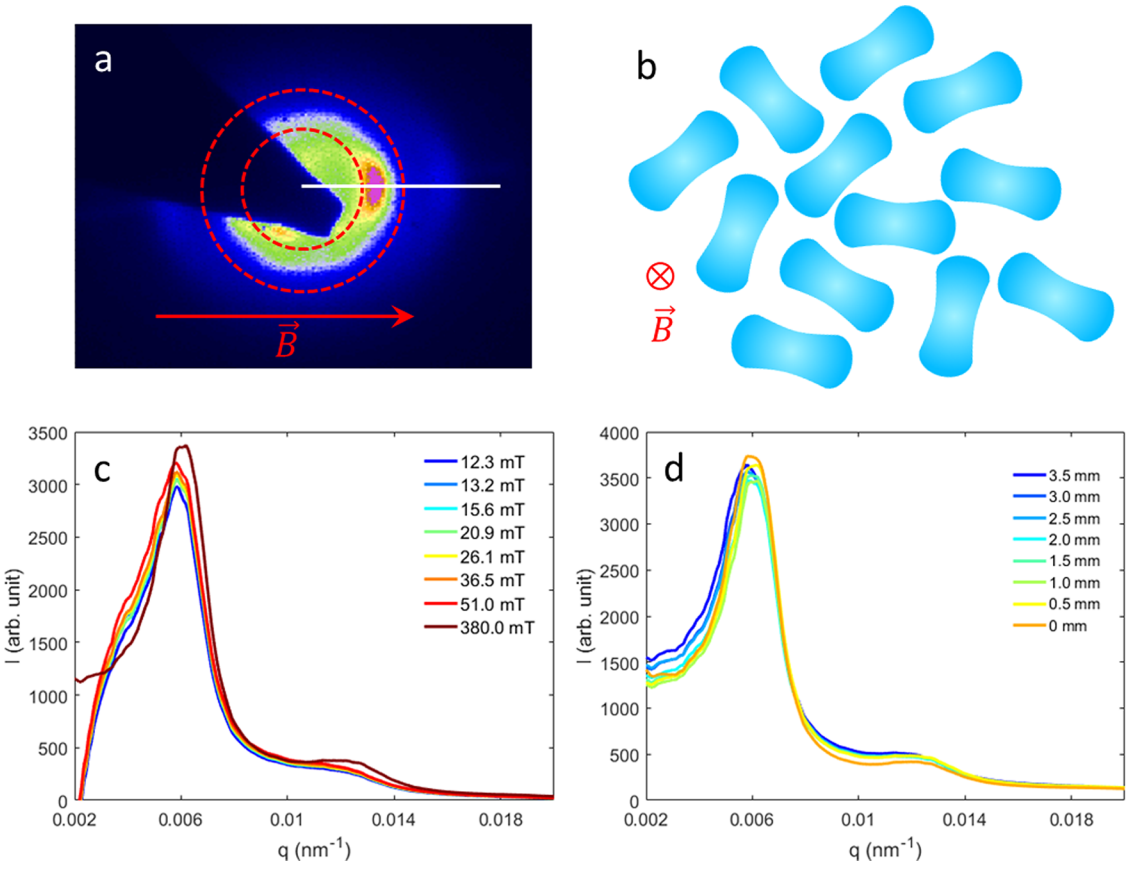

Figure 2. (a) Representative diffraction pattern for the nematic phase which was formed when the external field was applied after sedimentation. The azimuthal intensity profile has been calculated by taking an average of intensity lying between the red dashed lines. The intensity profile along the direction of the field has been calculated along the white line. (b) Schematic showing how the particles get aligned in the presence of an external field. One can notice that the short axes of the particles are fixed along the external field which is perpendicular to the plane of the paper while the long axes can still rotate around the field direction. This means that the nematic director is along the short axes of the particles indicating that it is oriented along the external field. Variation of the intensity profiles along the external field direction (along the white lines shown in (a)) (c) for different field values at a constant height Z = 2.0 mm from the bottom of the capillaries and (d) for different heights (Z) at a constant field B = 380 mT.

to be generic for rod-like anisotropic colloidal particles with hematite core. These observations can be rationalized by considering the fact that in both these cases the dipole moments lie in a plane perpendicular to the hematite c-axis which is parallel to the long axes of the particles.[11] As a result, in the presence of an external magnetic field the particles tend to align with their short axes parallel to the field direction. However, their long axes can still rotate around the magnetic field as shown in Figure 2b. This very peculiar arrangement of the dipole moments makes hematite ellipsoids and peanuts form *oblate* nematic phases in the presence of an external field in spite of the *prolate* shape of the particles.

The nearest neighbor distance, d, did not show any significant change when the magnitude of the magnetic field varied. Figure 2c shows the intensity profiles for different magnetic fields along the direction of the field shown by the white line in Figure 2a. Only at the maximum field (380 mT) does one find a slight shift in the peak position toward a higher q or lower d value. This indicates that at very high field value the resulting dipole−dipole attraction is significant, resulting in the formation of a more close-packed structure.

Due to the large size of the particles, their gravitational length, $L_g = k_BT/M_bg$ (k_BT being the thermal energy, M_b being the buoyant mass, and g being the gravitational acceleration), which is a measure of the balance between the thermal energy and the gravitational force, came out to be very small, ∼175 nm. As a result, dense sediments of the particles were formed, where gravitational compression occurred due to the mass of the particles lying above. Due to this very high gravitational compression, we did not observe any variation of the nearest neighbor distance as a function of height (Z) from the bottom of the capillaries (Figure 2d).

We have characterized the nematic phase by the orientational order parameter, S_2. Following Purdy et al.,[34,35] the azimuthal intensity distribution (between the red dotted lines in Figure 2a) can be fitted with

$$I = \text{baseline} + I_0 f(\omega) \tag{1}$$

where I_0 is the normalizing factor, ω is the azimuthal angle, and $f(\omega)$ is the orientational distribution function

$$f(\omega) = \exp(-AP(\omega)) \tag{2}$$

where the parameter A determines the width of the distribution function and $P(\omega)$ is the Legendre polynomial

$$P(\omega) = \frac{1}{2}(3\cos^2(\omega - \omega_0) - 1) \tag{3}$$

https://dx.doi.org/10.1021/acs.jpcb.0c03771
J. Phys. Chem. B 2020, 124, 5754−5760

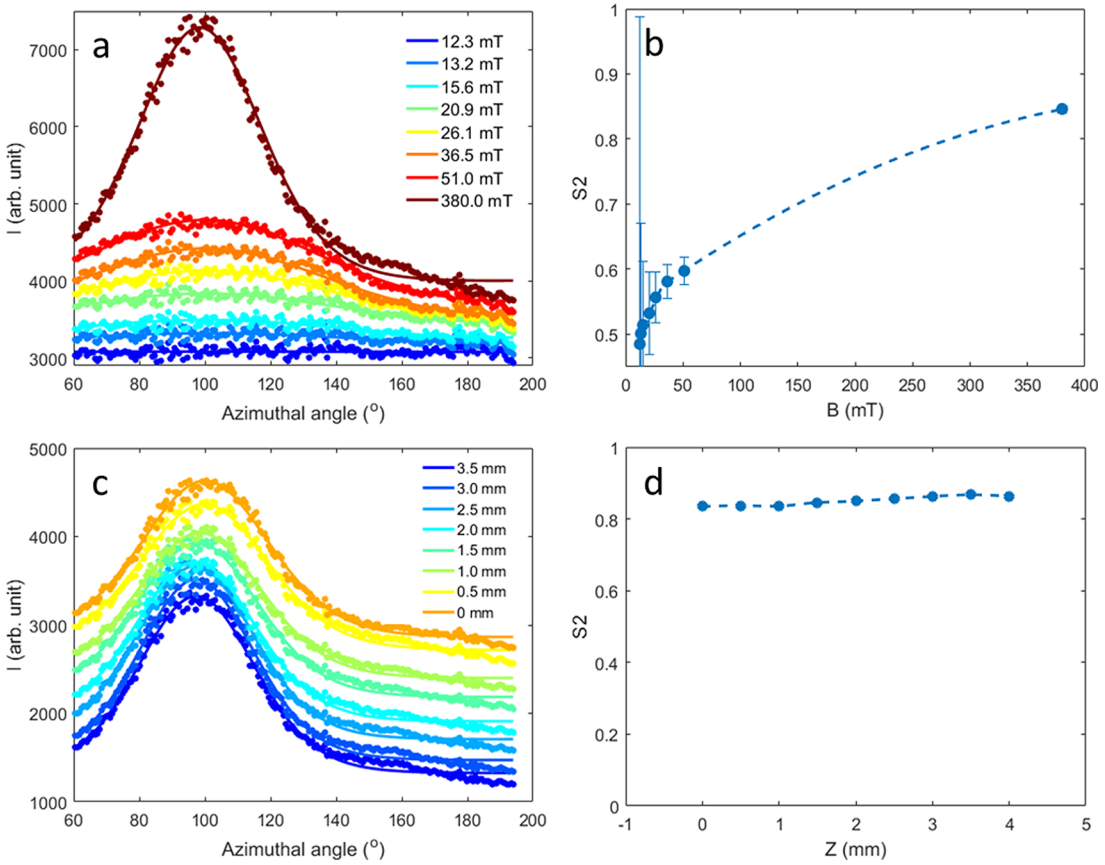

Figure 3. (a) Variation of azimuthal intensity profiles for different magnitudes of external field at a constant height Z = 2.0 mm. (b) Variation of orientational order parameter, S_2, as a function of external fields at Z = 2.0 mm. (c) Variation of azimuthal intensity profiles for different heights (Z) from the bottom of the capillaries at a constant magnetic field of B = 380 mT. (d) Variation of orientational order parameter, S_2, as a function of heights Z at a constant field B = 380 mT. In (a) and (c), symbols represent the experimental data while the continuous lines show the fitting with Purdy model. The graphs corresponding to different field values in (a) and heights in (c) are vertically shifted for better visualization. In (b) and (d), the dashed lines are guide to the eyes and not a fit.

where ω_0 is the tilt angle. The orientational order parameter, S_2, can now be obtained by

$$S_2 = \frac{\int f(\omega)P(\omega)\sin(\omega)\,d\omega}{\int f(\omega)\sin(\omega)\,d\omega} \quad (4)$$

Figure 3a shows the fit of the experimental data for different magnetic fields using the Purdy model, while Figure 3b represents the variation of S_2 as a function of magnetic field B at a particular height (Z = 2.0 mm) from the bottom of the capillaries. The analysis revealed that the orientational order develops as a function of the field strength, starting from a low value (<0.5), S_2 reaches a value of 0.85 at 380 mT. Similar analysis for the data at different heights of the capillaries indicate that there is not much variation of S_2 as a function of Z (Figure 3c,d).

Route 2: Application of the Magnetic Field *during* Sedimentation. In this case, the magnetic fields were applied soon after filling the capillaries with colloidal dispersion and continued during the sedimentation process. Figure 4a shows a representative diffraction pattern under this condition. An interesting feature that is obvious from the diffraction pattern is the anisotropy in the peaks perpendicular to the field direction. We have tried to come up with a plausible explanation in order to rationalize this observation by considering the fact that these particles form dipolar chains. These chains can in principle be considered as prolate objects that align along the field direction to form a para-nematic phase. They show a quasi-periodic structure along their axes, which is also the external field direction. However, in the perpendicular direction, they scatter up to $q_\perp \sim 2\pi/d_{\text{eff}}$, with d_{eff} being the effective diameter of the chains. Using SAXS data d_{eff} is found to be 1957 nm, which is in good agreement with the length of the particles. Further, the intensity profile along the direction of the field shows the appearance of a second-order peak (Figure 4b), the q value of which is double that of the first-order peak indicating the formation of a smectic phase. The nearest neighbor distance along this direction is found to be 1150 nm, which corresponds to the width of a single layer. We have used double Lorentzian function ($I = I_0 + (2A_1/\pi)\cdot(w_1/(4\times(q-q_{c1})^2 + w_1^2)) + (2A_2/\pi)\cdot(w_2/(4\times(q-q_{c2})^2 + w_2^2))$) to fit our experimental data and found the width of the first peak to be 0.0018 nm^{-1} indicating that around three layers are correlated. Surprisingly, just like the nematic phase (formed in the first case when the magnetic fields were applied after sedimentation), this smectic phase also has an oblate nature though the particles are prolate in shape.

To further probe the structure, we obtained the images of these self-assembled structures in real space using bright field microscopy. Representative bright field micrograph shown in Figure 4c proves that indeed under this particular condition these particles self-assembled into dipolar chains. In addition,

https://dx.doi.org/10.1021/acs.jpcb.0c03771
J. Phys. Chem. B 2020, 124, 5754−5760

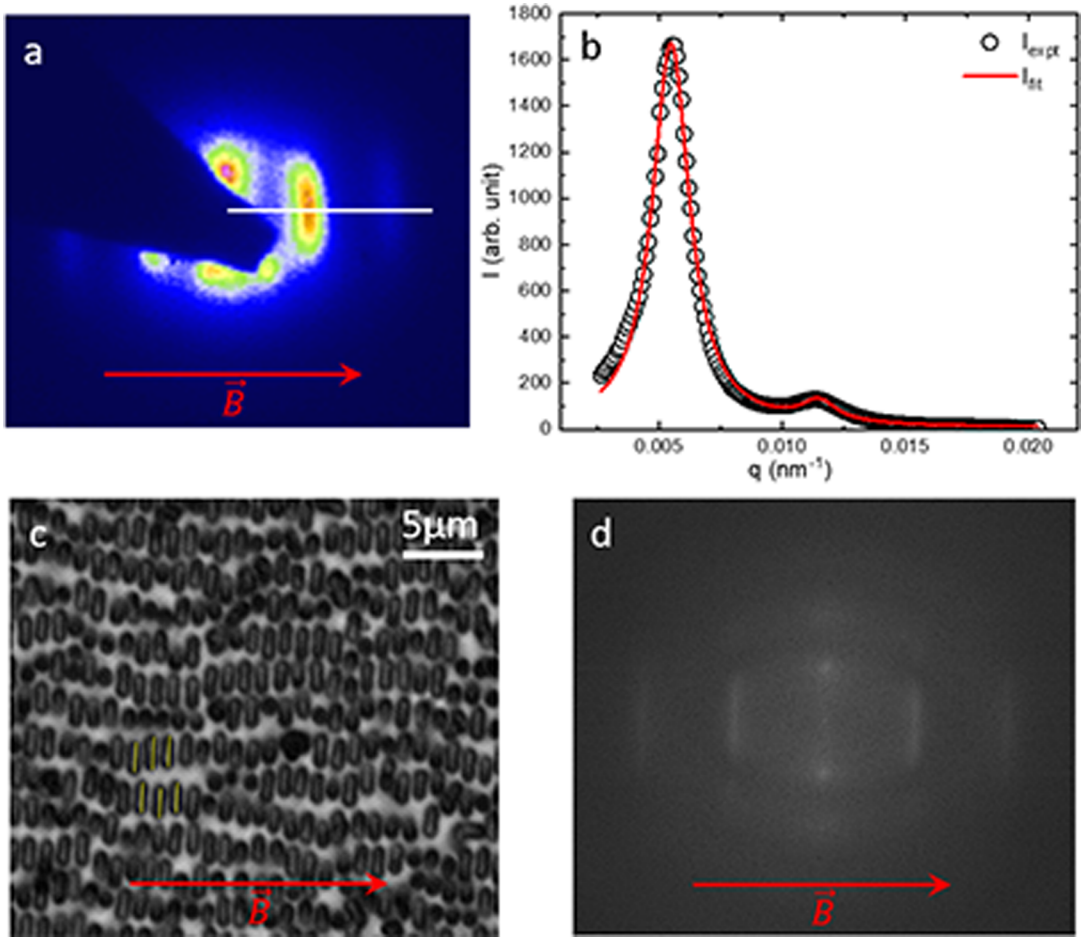

Figure 4. (a) Representative diffraction pattern for dipolar chains which were formed when the external field (30 mT) was applied during the sedimentation. (b) Intensity profile along the direction of the field; symbols represent the experimental data while the continuous line indicates the fitting with double Lorentzian function. (c) Representative bright field micrograph showing the dipolar chains in real space at B = 30 mT, and (d) it's FFT which qualitatively matches with (a). In (c), one can observe that within each chain particles can form layered structures as indicated by the yellow lines.

the qualitative resemblance of the fast Fourier transform (FFT) of the microscopic images (Figure 4d) with the diffraction patterns led us to the conclusion that the colloidal peanuts are indeed forming fluctuating dipolar chains while maintaining the short axes of the particles aligned along the magnetic fields. Further, a closer look at the internal structure of the individual chain reveals that inside each chain the particles are forming layered structures as indicated by yellow lines shown in Figure 4c (which is characteristics of smectic phase) with lots of defects. As already mentioned, as a signature of this smectic phase a second-order peak can be seen in the diffraction pattern (Figure 4a,b) as well as in the FFT (Figure 4d).

CONCLUSION

In conclusion, we have shown that one can tune the self-assembled structures formed by anisotropic magnetic colloidal peanuts in the presence of external magnetic field by changing the time of application of the external field. In the present case, depending on the time of application of the external field, two different self-assembled phases results. A nematic phase was obtained when the magnetic field was applied after the sedimentation process, while a phase made up of local dipolar chains resulted if the field was applied during the sedimentation process. Further, within each chain particles form smectic phase with lots of defects. Another interesting observation was that, although the particles are *prolate* in shape, the nematic and smectic phase formed by them has the characteristics of the one formed by *oblate* shaped particles. We believe this to be a generic feature for prolate-shaped, hematite anisotropic magnetic colloids with high dipolar moment. Our results will have direct implications in situations where manipulation of colloidal self-assembly using a external field will be employed as an alternative route toward the design of new materials. Our results indicate that it is not only important to study the final self-assembled structures but also the kinetic pathway leading to the final structures. Thus, acquired knowledge can be used to avoid metastable states while developing application oriented smart materials.

ASSOCIATED CONTENT

Supporting Information

The Supporting Information is available free of charge at https://pubs.acs.org/doi/10.1021/acs.jpcb.0c03771.

Representative diffraction pattern as well as intensity profiles corresponding to the isotropic phase formed in absence of an external field (PDF)

https://dx.doi.org/10.1021/acs.jpcb.0c03771
J. Phys. Chem. B 2020, 124, 5754−5760

AUTHOR INFORMATION

Corresponding Author

Antara Pal − *Division of Physical Chemistry, Department of Chemistry, Lund University, 22100 Lund, Sweden;* orcid.org/0000-0002-8998-6771; Email: antara.pal@fkem1.lu.se

Authors

Md. Arif Kamal − *Centre Interdisciplinaire de Nanoscience de Marseille (CINaM), CNRS, Aix-Marseille University, 13007 Marseille, France*

Andrei V. Petukhov − *Van't Hoff Laboratory for Physical and Colloid Chemistry, Utrecht University, 3512 JE Utrecht, The Netherlands;* orcid.org/0000-0001-9840-6014

Complete contact information is available at: https://pubs.acs.org/10.1021/acs.jpcb.0c03771

Notes

The authors declare no competing financial interest.

ACKNOWLEDGMENTS

The authors acknowledge Prof. Klas Flärdh for providing the optical microscope. Dr. Janne-Mieke Meijer is acknowledged for her help in synthesis. Dr. Daniel H. Merino is acknowledged for technical support during SAXS measurement in DUBBLE beamline in ESRF. Financial support from the European Research Council (Grant No. ERC-339678-COMPASS) and Netherlands Organization for Scientific Research (NWO) (700.10.355) is gratefully acknowledged. NWO is also acknowledged for providing the beamtime.

REFERENCES

(1) Sacanna, S.; Korpics, M.; Rodriguez, K.; Colón-Meléndez, L.; Kim, S.-H.; Pine, D. J.; Yi, G.-R. Shaping colloids for self-assembly. *Nat. Commun.* **2013**, *4*, 1688.

(2) Vlasov, Y. A.; Bo, X.-Z.; Sturm, J. C.; Norris, D. J. On-chip natural assembly of silicon photonic bandgap crystals. *Nature* **2001**, *414*, 289.

(3) Pal, A.; Malik, V.; He, L.; Erné, B. H.; Yin, Y.; Kegel, W. K.; Petukhov, A. V. Tuning the colloidal crystal structure of magnetic particles by external field. *Angew. Chem., Int. Ed.* **2015**, *54*, 1803−1807.

(4) Dinsmore, A. D.; Crocker, J. C.; Yodh, A. G. Self-assembly of colloidal crystals. *Curr. Opin. Colloid Interface Sci.* **1998**, 3, 5−11.

(5) Kuijk, A.; van Blaaderen, A.; Imhof, A. Synthesis of monodisperse, rodlike silica colloids with tunable aspect ratio. *J. Am. Chem. Soc.* **2011**, *133*, 2346−2349.

(6) Paineau, E.; Krapf, M.-E. M.; Amara, M.-S.; Matskova, N. V.; Dozov, I.; Rouziere, S.; Thill, A.; Launois, P.; Davidson, P. A liquid-crystalline hexagonal columnar phase in highly-dilute suspensions of imogolite nanotubes. *Nat. Commun.* **2016**, *7*, 10271.

(7) Lekkerkerker, H.; Vroege, G. Liquid crystal phase transitions in suspensions of mineral colloids: new life from old roots. *Philos. Trans. R. Soc., A* **2013**, *371*, 20120263.

(8) van der Kooij, F. M.; Kassapidou, K.; Lekkerkerker, H. N. Liquid crystal phase transitions in suspensions of polydisperse plate-like particles. *Nature* **2000**, *406*, 868.

(9) Malik, V.; Pal, A.; Pravaz, O.; Crassous, J. J.; Granville, S.; Grobety, B.; Hirt, A. M.; Dietsch, H.; Schurtenberger, P. Hybrid magnetic iron oxide nanoparticles with tunable field-directed self-assembly. *Nanoscale* **2017**, *9*, 14405−14413.

(10) Martchenko, I.; Crassous, J. J.; Mihut, A. M.; Bialik, E.; Hirt, A. M.; Rufier, C.; Menzel, A.; Dietsch, H.; Linse, P.; Schurtenberger, P. Anisotropic magnetic particles in a magnetic field. *Soft Matter* **2016**, *12*, 8755−8767.

(11) Lee, S. H.; Liddell, C. M. Anisotropic magnetic colloids: a strategy to form complex structures using nonspherical building blocks. *Small* **2009**, *5*, 1957−1962.

(12) Muangnapoh, K.; Avendaño, C.; Escobedo, F. A.; Watson, C. M. L. Degenerate crystals from colloidal dimers under confinement. *Soft Matter* **2014**, *10*, 9729−9738.

(13) Lee, S. H.; Gerbode, S. J.; John, B. S.; Wolfgang, A. K.; Escobedo, F. A.; Cohen, I.; Liddell, C. M. Synthesis and assembly of nonspherical hollow silica colloids under confinement. *J. Mater. Chem.* **2008**, *18*, 4912−4916.

(14) Hosein, I. D.; Lee, S. H.; Liddell, C. M. Dimer-based three-dimensional photonic crystals. *Adv. Funct. Mater.* **2010**, *20*, 3085−3091.

(15) Forster, J. D.; Park, J.-G.; Mittal, M.; Noh, H.; Schreck, C. F.; O'Hern, C. S.; Cao, H.; Furst, E. M.; Dufresne, E. R. Assembly of optical-scale dumbbells into dense photonic crystals. *ACS Nano* **2011**, *5*, 6695−6700.

(16) Pal, A.; Meijer, J.-M.; Wolters, J. R.; Kegel, W. K.; Petukhov, A. V. Structure and stacking order in crystals of asymmetric dumbbell-like colloids. *J. Appl. Crystallogr.* **2015**, *48*, 238−243.

(17) Henzie, J.; Grünwald, M.; Widmer-Cooper, A.; Geissler, P. L.; Yang, P. Self-assembly of uniform polyhedral silver nanocrystals into densest packings and exotic superlattices. *Nat. Mater.* **2012**, *11*, 131.

(18) Boneschanscher, M. P.; Evers, W. H.; Geuchies, J. J.; Altantzis, T.; Goris, B.; Rabouw, F. T.; Van Rossum, S.; van der Zant, H. S.; Siebbeles, L. D.; Van Tendeloo, G.; et al. Long-range orientation and atomic attachment of nanocrystals in 2D honeycomb superlattices. *Science* **2014**, *344*, 1377−1380.

(19) Miszta, K.; De Graaf, J.; Bertoni, G.; Dorfs, D.; Brescia, R.; Marras, S.; Ceseracciu, L.; Cingolani, R.; Van Roij, R.; Dijkstra, M.; et al. Hierarchical self-assembly of suspended branched colloidal nanocrystals into superlattice structures. *Nat. Mater.* **2011**, *10*, 872.

(20) Xu, X.; Friedman, G.; Humfeld, K. D.; Majetich, S. A.; Asher, S. A. Superparamagnetic photonic crystals. *Adv. Mater.* **2001**, *13*, 1681−1684.

(21) Xu, X.; Majetich, S. A.; Asher, S. A. Mesoscopic monodisperse ferromagnetic colloids enable magnetically controlled photonic crystals. *J. Am. Chem. Soc.* **2002**, *124*, 13864−13868.

(22) Chorny, M.; Fishbein, I.; Yellen, B. B.; Alferiev, I. S.; Bakay, M.; Ganta, S.; Adamo, R.; Amiji, M.; Friedman, G.; Levy, R. J. Targeting stents with local delivery of paclitaxel-loaded magnetic nanoparticles using uniform fields. *Proc. Natl. Acad. Sci. U. S. A.* **2010**, *107*, 8346−8351.

(23) Forbes, Z. G.; Yellen, B. B.; Barbee, K. A.; Friedman, G. An approach to targeted drug delivery based on uniform magnetic fields. *IEEE Trans. Magn.* **2003**, *39*, 3372−3377.

(24) Li, K. H.; Yellen, B. B. Magnetically tunable self-assembly of colloidal rings. *Appl. Phys. Lett.* **2010**, *97*, 083105.

(25) Yellen, B. B.; Hovorka, O.; Friedman, G. Arranging matter by magnetic nanoparticle assemblers. *Proc. Natl. Acad. Sci. U. S. A.* **2005**, *102*, 8860−8864.

(26) Mirica, K. A.; Shevkoplyas, S. S.; Phillips, S. T.; Gupta, M.; Whitesides, G. M. Measuring densities of solids and liquids using magnetic levitation: fundamentals. *J. Am. Chem. Soc.* **2009**, *131*, 10049−10058.

(27) Shapiro, N. D.; Mirica, K. A.; Soh, S.; Phillips, S. T.; Taran, O.; Mace, C. R.; Shevkoplyas, S. S.; Whitesides, G. M. Measuring binding of protein to gel-bound ligands using magnetic levitation. *J. Am. Chem. Soc.* **2012**, *134*, 5637−5646.

(28) Otsuka, K.; Wayman, C. Mechanism of shape memory effect and superelasticity. *Shape memory materials* **1998**, 27−48.

(29) Porter, D. A.; Easterling, K. E.; Sherif, M. *Phase Transformations in Metals and Alloys*, Revised Reprint; CRC press, 2009.

(30) Sugimoto, T.; Khan, M. M.; Muramatsu, A. Preparation of monodisperse peanut-type α-Fe2O3 particles from condensed ferric hydroxide gel. *Colloids Surf., A* **1993**, *70*, 167−169.

(31) Graf, C.; Vossen, D. L.; Imhof, A.; van Blaaderen, A. A general method to coat colloidal particles with silica. *Langmuir* **2003**, *19*, 6693−6700.

(32) Petukhov, A. V.; Meijer, J.-M.; Vroege, G. J. Particle shape effects in colloidal crystals and colloidal liquid crystals: Small-angle X-ray scattering studies with microradian resolution. *Curr. Opin. Colloid Interface Sci.* **2015**, *20*, 272−281.
(33) Bolhuis, P.; Frenkel, D. Tracing the phase boundaries of hard spherocylinders. *J. Chem. Phys.* **1997**, *106*, 666−687.
(34) Purdy, K. R.; Dogic, Z.; Fraden, S.; Rühm, A.; Lurio, L.; Mochrie, S. G. Measuring the nematic order of suspensions of colloidal fd virus by x-ray diffraction and optical birefringence. *Phys. Rev. E: Stat. Phys., Plasmas, Fluids, Relat. Interdiscip. Top.* **2003**, *67*, 031708.
(35) Kleshchanok, D.; Petukhov, A. V.; Holmqvist, P.; Byelov, D. V.; Lekkerkerker, H. N. Structures and phase behavior in mixtures of charged colloidal spheres and platelets. *Langmuir* **2010**, *26*, 13614−13621.

https://dx.doi.org/10.1021/acs.jpcb.0c03771
J. Phys. Chem. B 2020, 124, 5754−5760